

Stability and electronic structure of hydrogen passivated few atomic layer silicon films: A theoretical exploration

Shudong Wang, Liyan Zhu, Qian Chen, Jinlan Wang, and Feng Ding

Citation: *J. Appl. Phys.* **109**, 053516 (2011); doi: 10.1063/1.3553838

View online: <http://dx.doi.org/10.1063/1.3553838>

View Table of Contents: <http://jap.aip.org/resource/1/JAPIAU/v109/i5>

Published by the [American Institute of Physics](#).

Related Articles

Effect of indirect interband absorption in Ge/SiGe quantum wells

J. Appl. Phys. **110**, 083119 (2011)

Optical gain in short period Si/Ge superlattices on [001]-SiGe substrates

J. Appl. Phys. **110**, 083105 (2011)

Investigation of thermal transport degradation in rough Si nanowires

J. Appl. Phys. **110**, 074510 (2011)

Diffusion of E centers in germanium predicted using GGA+U approach

Appl. Phys. Lett. **99**, 072112 (2011)

Effective masses and electronic structure of diamond including electron correlation effects in first principles calculations using the GW-approximation

AIP Advances **1**, 032139 (2011)

Additional information on *J. Appl. Phys.*

Journal Homepage: <http://jap.aip.org/>

Journal Information: http://jap.aip.org/about/about_the_journal

Top downloads: http://jap.aip.org/features/most_downloaded

Information for Authors: <http://jap.aip.org/authors>

ADVERTISEMENT

**AIP**Advances

Submit Now

**Explore AIP's new
open-access journal**

- **Article-level metrics
now available**
- **Join the conversation!
Rate & comment on articles**

Stability and electronic structure of hydrogen passivated few atomic layer silicon films: A theoretical exploration

Shudong Wang,¹ Liyan Zhu,¹ Qian Chen,¹ Jinlan Wang,^{1,2,a)} and Feng Ding^{3,b)}

¹Department of Physics, Southeast University, Nanjing, 211189, China

²School of Chemistry and Chemical Engineering, Southeast University, Nanjing, 211189, China

³Institute of Textiles and Clothing, Hong Kong Polytechnic University, Kowloon, Hong Kong

(Received 7 November 2010; accepted 4 January 2011; published online 14 March 2011)

The stability, electronic, and optical properties of two dimensional hydrogenated few atomic layer silicon (H-FLSi) are systematically studied with density functional theory calculations. The formation energy of H-FLSi decreases with increasing layer thickness and approaches zero at the thickness of double layer, suggesting that this material is energetically favorable and thus its experimentally synthesizing is feasible. Its bandgap decreases with the increase of the thickness and eventually approaches the value of bulk silicon. More interestingly, the bandgap of hydrogenated silicon films can be tuned by external electric field and even becomes metal. Importantly, the light absorption threshold and absorption peak of the H-Si mono- and bilayer locate in different energy regions and both move toward higher energy region as compared with those of the bulk silicon. © 2011 American Institute of Physics. [doi:10.1063/1.3553838]

I. INTRODUCTION

Graphene, a one atom layer thick two dimensional (2D) material, attracts enormous interests in physics, material science, and chemistry because of its unique mechanical, chemical and electronic properties related to its specific 2D crystal structure.¹⁻⁷ While, a perfect graphene has zero bandgap at the Dirac points in the Brillouin zone,^{8,9} which makes it not an ideal semiconducting material as silicon for electronic application.

Just beneath C in the periodic table, Si has very different structural and electronic properties. Bulk Si has a medium bandgap, 1.2 eV, which makes it the fundamental semiconducting material. Free standing one atom thick 2D Si is not as stable as graphene because sp^3 hybridized Si is more stable than sp^2 hybridized Si, which is opposite to C. However, a one atom thick Si layer can be stabilized by hydrogenation on both sides. Experimentally, Dahn *et al*¹⁰ have successfully synthesized hydrogen passivated monolayer silicon (named as layered polysilane in the chemical formula of SiH). The layered polysilane has hexagonal structure with an in-plane lattice constant of 3.83 Å and the distance between neighboring layers is 5.4 Å. Theoretically, Takeda *et al*¹¹ have investigated the electronic structure of silicon skeleton chainlike (one-dimensional, 1D), planar 2D and 3D crystalline and found 2D polysilane has a mixed bandgap structure consisting of a direct one (2.48 eV) and an indirect one (2.63 eV) which is an intermediate between 1D (the direct gap) and 3D (the indirect gap). Van de Walle *et al*¹² have revealed that an isolated layer of SiH compound has a large, nearly direct bandgap of 2.75 eV with very strong direct transitions.

Beyond the one atom thick 2D system, films of finite silicon layers thickness have also been studied.¹³ Tse *et al*¹³

have found that the layered Si_6nH_6 have a weak indirect bandgap decreasing and approaching the bulk silicon one as increasing of the layers. In this article, we revisit the hydrogenated few atomic layer thick silicon films and systematically study their stability, electronic, and optical properties. We find that both the direct and the indirect bandgap decreases with the layer thickness. We also find that the bandgap of these Si films decreases with an increasing applied electric field and is eventually closed at electric field greater than ~ 0.9 V/Å. More interestingly, the optical property of H-FLSi is thickness dependent. The absorption peaks continuously move to high energy region with the thickness decreasing. The continuous change of light absorption peaks suggests that laying H-FLSi of various thicknesses together can be used as the broad spectrum light absorption agent in silicon based solar cells.

II. COMPUTATIONAL METHOD

The calculations of geometric and electronic structures of H-FLSi are carried out by first-principle density functional theory (DFT) calculations implemented within the Vienna Ab initio Simulation Package (VASP).¹⁴ We exploit the Perdew, Burke, and Ernzerhof (PBE)¹⁵ exchange–correlation potentials and projected augmented wave (PAW).¹⁶ The energy cutoff is 400 eV and the vacuum space perpendicular to the two-dimensional layers is larger than 15 Å to avoid interaction between neighboring sheets. The Brillouin zone integration is done by $15 \times 15 \times 1$ and $19 \times 19 \times 1$ k -point meshes in structure optimization and static electronic structure calculations, respectively. Conjugated gradient algorithm is adopted in the structure optimizations until the Hellmann-Feynman forces acting on each atom are smaller than 0.01 eV/Å. The convergence criterion for energy is 10^{-4} eV. We further verify the hydrogenated monolayer and bilayer Si films are local minima rather than transition states through exploit phonon dispersion calculation implemented

^{a)}Electronic mail: jlwang@seu.edu.cn.

^{b)}Electronic mail: tcfding@inet.polyu.edu.hk.

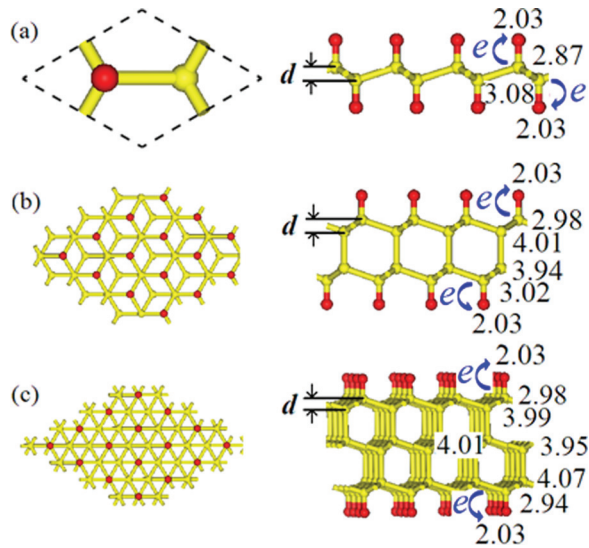


FIG. 1. (Color online) Structure of hydrogenated few layer silicon (H-FLSi): (a) monolayer, (b) bilayer and (c) trilayer. Each of them has a top view (left column) and a side view (right column). The dashed line marked area is unit cell of our calculations. Charge population is given for the three structures. The arrow denotes the direction of electrons transference. Si atoms are shown in yellow (grey) and H atoms are shown in red (black).

in QUANTUM-ESPRESSO code,¹⁷ which all the frequencies in these two systems are positive.

To explore the difference in the optical properties among the bulk silicon, hydrogenated silicon mono- and bilayer, we perform first-principles calculations using a many-body perturbation theory through three steps. First, we re-optimize the ground-state electronic properties of these systems, by using the local density approximation (LDA)¹⁸ and norm-conserving pseudopotentials,¹⁹ implemented in QUANTUM-ESPRESSO code. Then, electronic quasiparticle corrections are calculated within the *GW* approximation to the exchange-correlation self-energy, where the LDA wave functions are used as good approximations for the quasiparticle ones, and the screening is treated within the plasmon-pole approximation.²⁰ Finally, the Bethe-Salpeter equation is solved for obtain the absorption spectrum. Moreover, only the case of in-plane polarization is considered in the calculations. The second and third steps were performed with YAMBO code.²¹

III. RESULTS AND DISCUSSION

A. Structure and stability

First, we study the structure of the hydrogenated few layer silicon (H-FLSi) films. Each H-FLSi composes a film of one or a few parallel corrugated hexagonal silicon planes. Hydrogen atoms are placed on both top and bottom of the silicon film to passivate the dangling sp^3 σ bonds on the surface. Relaxed structures of the hydrogenated mono-, bi- and tri-layer Si are shown in Fig. 1. For hydrogenated monolayer Si, each unit cell contains two silicon atoms and two hydrogen atoms. The Si-Si bond length is 2.36 Å, similar to the value of Si bulk calculated by same method (2.35 Å). The Si-H bond length is 1.50 Å. These values are also in good agreement with the previous theoretical result.²² As clearly seen from Table I, the intralayer Si-Si bond length is slightly shorter than that of interlayer, indicating that the intralayer interaction is relatively stronger than the interlayer interaction. Each silicon atomic layer consists of two subplanes, which is separated by a distance d . The distance d in the monolayer Si is only 0.715 Å, $\sim 9\%$ smaller than in the bulk value of 0.784 Å. The distance d increases gradually to 0.762 Å at the thickness of eight layers and converges to the value of bulk Si. Bader charge analysis of the hydrogenated mono-, bi- and tri-layer silicon is shown in Fig. 1. As it can be seen from the figure, hydrogen atoms notably gain electrons from the nearest silicon atoms because of the strong electro-negativity of hydrogen atom.

The stability of H-FLSi is evaluated by formation energy (FE) of H-FLSi. The definition of FE is:

$$FE = [E_{Si+H} - N_{Si}E_{Si} - N_H(E_{H_2}/2)]/N_{Si}, \quad (1)$$

where E_{Si} and E_{H_2} are energies of silicon atom in bulk Si and hydrogen molecule, respectively; N_i ($i = Si, H$) is the number of silicon (hydrogen) atoms; E_{Si+H} is the total energy of H-FLSi. Figure 2 shows the formation energy of H-FLSi as a function of number of Si layers. Clearly, the formation energy of the H-FLS decreases with the film thickness. The very small positive formation energy (0.015 eV) of the monolayer H-FLSi indicates that it is less stable than the multilayer ones. The increasing negative formation energy of the multilayer films indicates their increased stability.

TABLE I. Intralayer and interlayer Si-Si bond lengths (unit in Å), formation energy per silicon atom (unit in eV), and band gap (unit in eV) of H-FLSi.

Number of Layers	Intralayer Si-Si bond length	Interlayer Si-Si bond length	Formation Energy	Band Gap	
				Direct	Indirect
1	2.362	–	0.015	2.328	2.186
2	2.356	2.361	–0.008	1.986	1.435
3	2.362	2.364	–0.021	1.737	1.149
4	2.361	2.365, 2.360	–0.028	1.651	1.006
5	2.360–2.368	2.363–2.366	–0.032	1.605	0.917
6	2.359–2.368	2.364–2.360	–0.034	1.573	0.860
7	2.360–2.369	2.365–2.369	–0.036	1.546	0.806
8	2.360–2.369	2.365–2.369	–0.038	1.529	0.784
Bulk Si				indirect gap: 0.635	

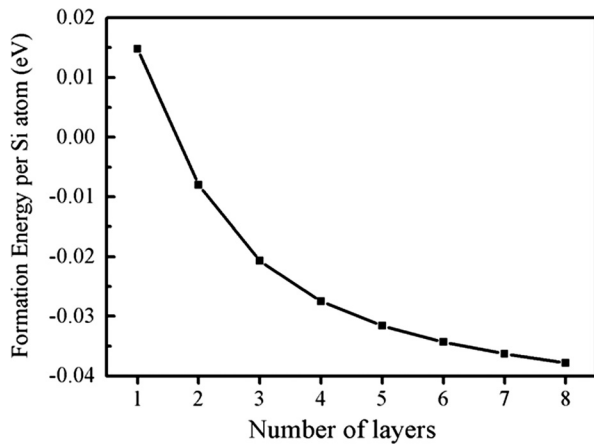


FIG. 2. Formation energy of H-FLSi per silicon atom corresponds to the number of layers.

B. Electronic structures with and without an external electric field

The band structures of H-FLSi of different thickness exhibit similar features, that is, all the structures have a conduction band minimum (CBM) near the M point and a valence band maximum (VBM) at the Γ point [Figs. 3(a) and 3(b)]. Namely, all H-FLSi films maintain the electronic property of indirect bandgap of bulk silicon. As thickness increases, both the direct and indirect band gaps decrease monotonically and converge to the value of bulk silicon [Fig. 3(c)], in agreement with the value of Ref. 13. However, the dependence of the direct and indirect bandgap on the number of layers is different. The indirect bandgap decreases much more dramatically than the direct one with increasing thickness, which suggests that the quantum confinement effect has more significant impact on the indirect bandgap. Hence, we can manipulate the bandgap and electronic structure by varying the thickness. This is very different from that of layered siloxene (in which HO groups substitute H atoms). Hirayama *et al.*²³ found that the direct gap of layered siloxene is dominated by the surface states while the indirect gap is dominated by the quantum confinement effect. Thus the direct gap cannot be changed by varying the thickness. Comparison of the DOS of hydrogen-

ated mono-, bi-, tri-layer Si, and the bulk Si [Fig. 3(d)] shows that the localized peak (the sharp peak in the figures) goes weaker with the increasing thickness and moves toward lower energy range, indicating that electrons in the fewer layers are more localized than the more layer ones.

Figure 4 presents the density of states (DOS) of the hydrogenated bilayer Si and the insert depicts the partial charge densities of the CBM and VBM. The DOS clearly shows that the p_x and p_y states are degenerated due to the D_{3d} symmetry of the system. The Si $3p_z$ states, perpendicular to the silicon plane, hybridize with H $1s$ states to stabilize the structure. The partial charge densities suggest the VBM of H-FLSi mainly contributes from the intralayer Si-Si bonding states, which can also be reflected from the DOS. Whereas the conduction band at the Γ point has the anti-bonding characteristic between the intralayer Si atoms, but is of bonding feature between the interlayer Si atoms. Therefore, the charge density distribution of CBM is not only in surface but also toward the interior. Thus, the conduction bands of H-FLSi show great dependence on the thickness of the H-FLSi.

Applying external electric field has been proved an efficient mean of tuning electronic structure of low dimensional nanomaterials.^{24–27} Here we explore the bandgap variation of H-FLSi films in external electric field. An external electric field from 0 to 1.0 V/Å is applied along the direction perpendicular to the basal plane. The band structures of the hydrogenated bilayer Si film with $E = 0, 0.8$ and 0.9 V/Å are presented in Figs. 5(a)–5(c), respectively. The conduction bandedge significantly shifts downwards and the bandgap becomes narrower and narrower (which means enhanced metallicity) as increasing the electric field. Figs. 5(d) and 5(e) present the partial charge densities of CBM at $E = 0$ and 0.9 V/Å, respectively. Without electric field applied, the CBM of the bilayer Si is localized. While the CBM becomes delocalized at $E = 0.9$ V/Å. When $E = 0$ V/Å, the direct and indirect band gaps are 1.99 eV and 1.44 eV, respectively. At $E = 0.8$ V/Å, the indirect bandgap drops dramatically and the system is turned from an indirect-gap semiconductor into a direct-gap one with a direct gap of 1.16 eV. Further increasing the electric field to 0.9 V/Å, the system is eventually

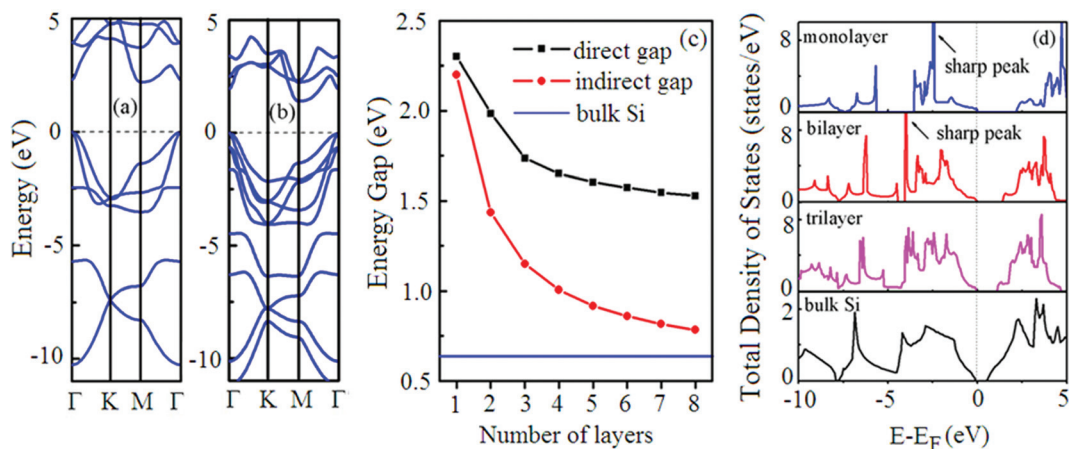


FIG. 3. (Color online) Band structures of the (a) monolayer and the (b) bilayer H-Si; (c) direct and indirect band gaps of H-FLSi, horizontal line referring to our calculated direct bandgap of bulk silicon; (d) total DOS of the hydrogenated Si mono-, bi-, tri-layers and bulk silicon. The Fermi level is set to be zero.

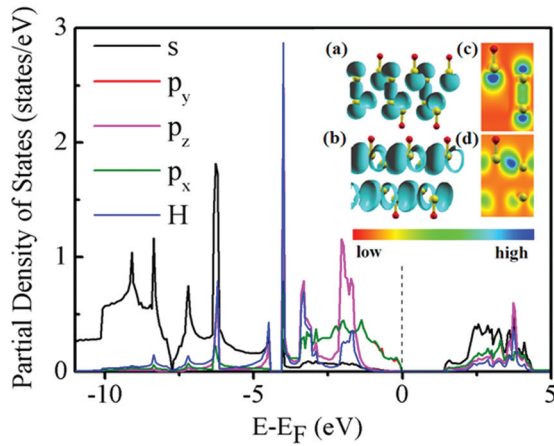


FIG. 4. (Color online) DOS of the hydrogenated Si bilayer. The inset is charge densities of the (a) conducting and (b) valence bands at Γ point; (c) and (d) are two-dimensional plots corresponding to the conduction and valence bands, respectively.

converted into a conductor [Fig. 5(f)]. The conduction band edge (CBE) at gamma point has a vertical character [Fig. 4(a)], so the external electric field perpendicular to the basal plane, which redistributes the charge mainly along the electric field direction, makes the CBE at gamma dramatically downshift. It should be noted that the DFT calculation always underestimates the bandgap, but it is powerful to predict a correct trend toward the bandgap change and to properly demonstrate the physical mechanism.^{28,29} The total charge density difference is defined as

$$\Delta\sigma = \sigma(E) - \sigma(0), \quad (2)$$

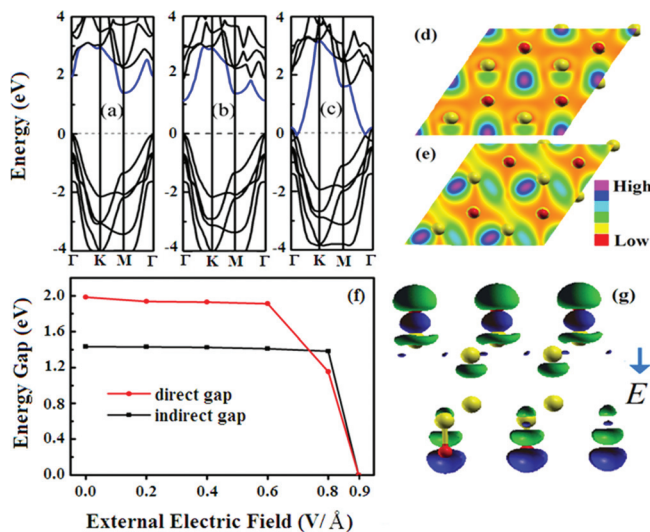


FIG. 5. (Color online) Band structures of the hydrogenated bilayer with an external electric field $E =$ (a) 0, (b) 0.8 and (c) 0.9 $\text{V}/\text{\AA}$, respectively. The Fermi level is set to be zero, and the conducting band is plotted with blue (grey) line. The charge densities of the conducting band minimum under an external electric field $E =$ (d) 0, (e) 0.9 $\text{V}/\text{\AA}$, respectively. (f) bandgap as a function of external electric field. (g) total charge density difference of the hydrogenated Si bilayer induced by $E = 0.8 \text{ V}/\text{\AA}$ from up to down with an isosurface value of $\pm 0.003 e/\text{\AA}^3$. Green (grey)/blue (black) region represents electron accumulation/depletion.

where $\sigma(0)$ and $\sigma(E)$ are the charge density of the hydrogenated bilayer Si without electric field and under a specific electric field E , respectively. The total charge density difference $\Delta\sigma$ of the bilayer at $E = 0.8 \text{ V}/\text{\AA}$ is given in Fig. 5(g). This electric field induces the charge accumulation (green area) and charge depletion (blue area) on the surface. The field-induced charge redistribution results in the great variation in electronic structures of H-FLSi. Our calculations suggest that the external electric field can lead to a transition from a wide indirect gap semiconductor to a direct one, and even to a conductor.

C. Optical properties

According to the above discussion, the hydrogenated few atom layer Si films have quite different electronic structure from the bulk silicon, which must result in very different optical properties. The optical absorption spectra of bulk silicon, hydrogenated silicon mono- and bilayer are displayed in Fig. 6. The two absorption peaks of bulk silicon lie at 3.38 eV and 4.04 eV, respectively, both in good agreement with the experiment values of 3.49 eV and 4.33 eV.³⁰ For the H-Si mono- and bilayer, the two peaks move toward higher energy region (blue-shift). The first absorption peak of the H-Si monolayer (bilayer) moves to 4.38 (4.04 eV). The absorption threshold of the monolayer is higher than that of bilayer's, and it moves toward the bulk value as the film thickness increasing. The continuous change of light absorption spectrum and the different peak positions are of great interest for solar cell application. In solar cell technology, normally multi-layered light absorbers with different absorption peaks are stacking together to ensure an efficient light absorption. While the multi-layer stacking increases the thickness of the p-n junction and thus the rate of the electron-hole recombination would be significantly increased as well. These H-FLSi films are only 1 or a few nm thick and their absorption peaks can be tuned continuously. So they can be used as efficient light absorbers in solar cells, especially in the widely used silicon based solar cells.

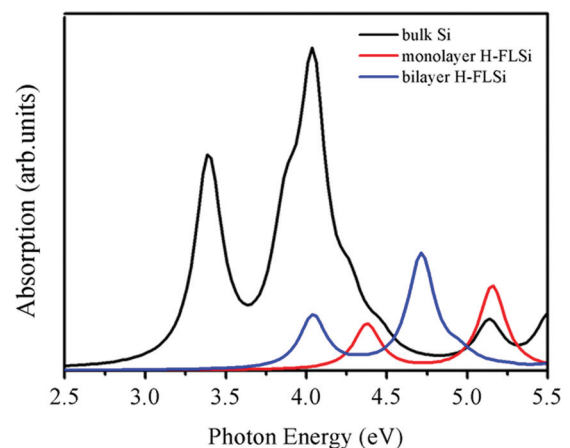


FIG. 6. (Color online) Optical absorption spectra of bulk silicon, the mono and bilayers hydrogenated Si. [black: bulk silicon; red (dark grey): monolayer; blue (light grey): bilayer].

IV. CONCLUSIONS

In summary, we have systematically studied the stability, electronic, and optical properties of hydrogenated few layer silicon films. The stability of H-FLSi films increases with the increasing thickness. The direct and indirect bandgap can be tuned from 2.328 eV and 2.186 eV to the bulk silicon by varying the thickness of H-FLSi. The layer thickness dependence bandgap behavior can also be modulated by external electric field. For the H-Si bilayer, a transition from semiconductor to metal occurs at the electric field of 0.9 V/Å. Moreover, both the light absorption threshold and peaks of H-FLSi films are blue-shift in comparison with those of the bulk silicon. This suggests that laying H-FLSi of various thicknesses together can be used as wide spectrum light absorption agent in silicon based solar cell application.

ACKNOWLEDGMENTS

This work is supported by the NSF (11074035, 20873019), NBRP (2010CB923401, 2011CB302004, 2009CB623200), SRFDP (20090092110025), and Peiyu Foundation of SEU. The computation work is done using a computational facility at Department of Physics, Southeast University.

- ¹K. S. Novoselov, A. K. Geim, S. V. Morozov, D. Jiang, Y. Zhang, S. V. Dubonos, I. V. Grigorieva, and A. A. Firsov, *Science* **306**, 666 (2004).
²K. S. Novoselov, D. Jiang, F. Schedin, T. J. Booth, V. V. Khotkevich, S. V. Morozov, and A. K. Geim, *Proc. Natl. Acad. Sci. U.S.A.* **102**, 10451 (2005).
³Y. W. Son, M. L. Cohen, and S. G. Louie, *Phys. Rev. Lett.* **97**, 216803 (2006).

- ⁴S. Stankovich, D. A. Dikin, G. H. B. Dommett, K. M. Kohlhaas, E. J. Zimney, E. A. Stach, R. D. Piner, S. T. Nguyen, and R. S. Ruoff, *Nature* **442**, 282 (2006).
⁵A. K. Geim and K. S. Novoselov, *Nat. Mater.* **6**, 183 (2007).
⁶A. H. Castro Neto, F. Guinea, N. M. R. Peres, K. S. Novoselov, and A. K. Geim, *Rev. Mod. Phys.* **81**, 109 (2009).
⁷L. Y. Zhu, J. L. Wang, T. T. Zhang, L. Ma, C. W. Lim, F. Ding, and X. C. Zeng, *Nano Lett.* **10**, 494 (2010).
⁸P. R. Wallace, *Phys. Rev.* **71**, 622 (1974).
⁹J. W. McClure, *Phys. Rev.* **104**, 666 (1956).
¹⁰J. R. Dahn, B. M. Way, E. Fuller, and J. S. Tse, *Phys. Rev. B* **48**, 17872 (1993).
¹¹K. Takeda and K. Shiraishi, *Phys. Rev. B* **39**, 11028 (1989).
¹²C. G. Van de Walle and J. E. Northrup, *Phys. Rev. Lett.* **70**, 1116 (1993).
¹³J. S. Tse, J. R. Dahn, and F. Buda, *J. Phys. Chem.* **99**, 1896 (1995).
¹⁴G. Kresse and J. Hafner, *Phys. Rev. B* **47**, 558 (1993).
¹⁵J. P. Perdew, K. Burke, and M. Ernzerhof, *Phys. Rev. Lett.* **77**, 3865 (1996).
¹⁶P. E. Blochl, *Phys. Rev. B* **50**, 17953 (1994).
¹⁷S. Baroni, A. D. Corso, S. de Gironcoli, P. Giannozzi, C. Cavazzoni, G. Ballabio, S. Scandolo, G. Chiarotti, P. Focher, A. Pasquarello, K. Laasonen, A. Trave, R. Car, N. Marzari, and A. Kokalj, available at <http://www.pwscf.org>.
¹⁸D. M. Ceperley and B. J. Alder, *Phys. Rev. Lett.* **45**, 566 (1980).
¹⁹N. Troullier and J. L. Martins, *Phys. Rev. B* **43**, 1993 (1991).
²⁰R. W. Godby and R. J. Needs, *Phys. Rev. Lett.* **62**, 1169 (1989).
²¹A. Marini, C. Hogan, M. Gruning, and D. Varsano, *Comput. Phys. Comm.* **180**, 1392 (2009).
²²N. Lu, Z. Y. Li, and J. L. Yang, *J. Phys. Chem. C* **113**, 16741 (2009).
²³M. Hirayama, J. Nakamura, and A. Natori, *E.-J. Surf. Sci. Nanotechnol.* **4**, 528 (2006).
²⁴J. O'Keeffe, C. Y. Wei, and K. J. Cho, *Appl. Phys. Lett.* **80**, 676 (2002).
²⁵K. H. Khoo, M. S. C. Mazzoni, and S. G. Louie, *Phys. Rev. B* **69**, 201401(R) (2004).
²⁶J. Neugebauer and M. Scheffler, *Phys. Rev. B* **46**, 16067 (1992).
²⁷P. J. Feibelman, *Phys. Rev. B* **64**, 125403 (2001).
²⁸Y. W. Son, M. L. Cohen, and S. G. Louie, *Nature* **444**, 347 (2006).
²⁹Z. Zhang and W. Guo, *Phys. Rev. B* **77**, 075403 (2008).
³⁰P. Lautenschlager, M. Garriga, L. Vina, and M. Cardona, *Phys. Rev. B* **36**, 4821 (1987).